G. R. Library

2

MARTIN MARIETTA ENERGY SYSTEMS LIBRARIES

3 4456 0364473 2

ORNL-3221
UC-25 – Metals, Ceramics, and Materials
TID-4500 (16th ed., Rev.)

FEASIBILITY STUDIES – NONDESTRUCTIVE TESTING OF THE ENRICO FERMI REACTOR CORE B FUEL ELEMENT

R. W. McClung

CENTRAL RESEARCH LIBRARY
DOCUMENT COLLECTION
LIBRARY LOAN COPY
DO NOT TRANSFER TO ANOTHER PERSON
If you wish someone else to see this document, send in name with document and the library will arrange a loan.

OAK RIDGE NATIONAL LABORATORY
operated by
UNION CARBIDE CORPORATION
for the
U.S. ATOMIC ENERGY COMMISSION

Printed in USA. Price $1.00. Available from the
Office of Technical Services
Department of Commerce
Washington 25, D.C.

LEGAL NOTICE

This report was prepared as an account of Government sponsored work. Neither the United States, nor the Commission, nor any person acting on behalf of the Commission:

A. Makes any warranty or representation, expressed or implied, with respect to the accuracy, completeness, or usefulness of the information contained in this report, or that the use of any information, apparatus, method, or process disclosed in this report may not infringe privately owned rights; or

B. Assumes any liabilities with respect to the use of, or for damages resulting from the use of any information, apparatus, method, or process disclosed in this report.

As used in the above, "person acting on behalf of the Commission" includes any employee or contractor of the Commission, or employee of such contractor, to the extent that such employee or contractor of the Commission, or employee of such contractor prepares, disseminates, or provides access to, any information pursuant to his employment or contract with the Commission, or his employment with such contractor.

ORNL-3221

Contract No. W-7405-eng-26

METALLURGY DIVISION

FEASIBILITY STUDIES – NONDESTRUCTIVE TESTING OF THE ENRICO FERMI REACTOR CORE B FUEL ELEMENT

R. W. McClung

DATE ISSUED

DEC 21 1961

OAK RIDGE NATIONAL LABORATORY
Oak Ridge, Tennessee
operated by
UNION CARBIDE CORPORATION
for the
U. S. ATOMIC ENERGY COMMISSION

MARTIN MARIETTA ENERGY SYSTEMS LIBRARIES
3 4456 0364473 2

FEASIBILITY STUDIES – NONDESTRUCTIVE TESTING OF THE ENRICO FERMI REACTOR CORE B FUEL ELEMENT

R. W. McClung

ABSTRACT

This report discusses a series of feasibility studies which were conducted to determine the capabilities and limitations of several nondestructive testing methods as applied to the Core B fuel element of the Enrico Fermi Fast Breeder Reactor. An eddy-current technique is demonstrated to be capable of measuring the fuel plate-clad thickness with an accuracy of ± 0.001 in. Discussion is presented of a through-transmission ultrasonic technique which is capable of detecting core-clad interface nonbonds which are 1/8 in. in diameter or larger. A radiographic technique is described which can be used to detect UO_2 concentration inhomogeneities in excess of the specified ± 5% tolerance. Description is made also of an eddy-current system which will measure coolant channel spacing between fuel plates with an accuracy of 0.0005 in. Details of each of the test systems are presented.

INTRODUCTION

As part of an integrated materials program to develop a UO_2-stainless steel dispersion fuel element for Core B of the Enrico Fermi Fast Breeder Reactor, a series of studies have been conducted to determine the applicability of nondestructive techniques for measuring certain desired properties in the element. These studies were not intended to culminate in the complete development of techniques and systems but, rather, were to determine capabilities and limitations of several testing methods as applied to the Fermi element. The data thus collected should be of value in the preparation of purchase specifications, and as a guide to prospective fuel fabricators.

The proposed Core B fuel element, shown in Fig. 1, is composed of a series of parallel flat fuel plates brazed into a box-like array with 0.054-in. coolant channels between each plate. The plates themselves are approx 19 in. long, 0.115 in. thick, and 2.4 in. wide. The core material is composed of approx 35 wt %

UNCLASSIFIED
ORNL-LR-DWG 53039A

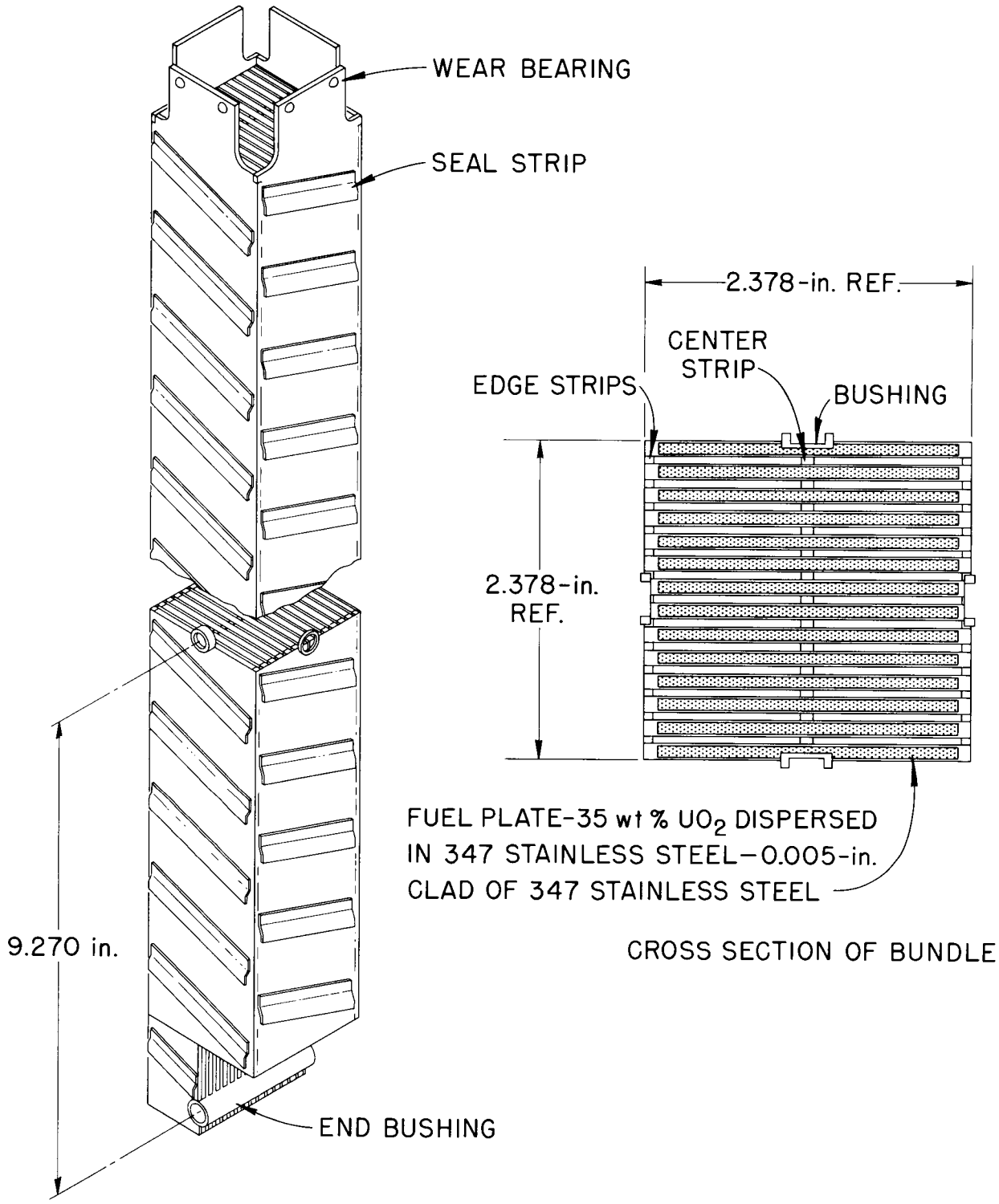

Fig. 1. Core B Fuel Subassembly — Fermi Reactor.

spheroidal UO_2 particles dispersed in type 347 stainless steel. This core is enclosed within a frame of type 347 stainless steel and clad with approx 0.005 in. of the same material. Plates are fabricated by the conventional picture-frame technique.

The original areas of investigation were:

1. A study of eddy-current techniques for the measurement of clad thickness over the core material;

2. A study of ultrasonic techniques for the detection of nonbond areas between the core and clad; and

3. A study of radiographic techniques for the determination of inhomogeneities in UO_2 loading.

A later request was for techniques to measure the coolant channel spacing between the plates of the assembled fuel elements.

Each of these four areas of development is separately discussed in the following sections of this report.

EDDY-CURRENT MEASUREMENT OF CLAD THICKNESS

Purpose

It is desirable and generally mandatory to operate a nuclear reactor with a minimum of radioactive contamination in the coolant resulting from the release of fissionable materials or fission by-products. The common method of preventing such release is to shroud the fissionable material so that complete containment is achieved. The Core B fuel plate has an 0.005-in.-thick type 347 stainless steel clad as an integral part of the plate structure. A thicker cladding is undesirable, since one of the design objectives is to incorporate the maximum amount of UO_2 without exceeding limits of existing technology. A minimum thickness of clad is obviously required to provide assurance that minor corrosive or erosive attack will not result in excessive contamination of the sodium coolant. For these reasons, close control is necessary to ensure that the specified clad thickness is present. The design of this fuel plate specifies an average clad thickness of 0.005 ± 0.001 in. with the minimum allowable at any point being 0.003 in.

Theory

The eddy-current method[1,2] was chosen as the best approach to the solution of this measuring problem. If a coil of wire is energized with a high-frequency electrical signal, it will have a characteristic impedance and will generate a magnetic field. If an electrical conductor is brought into this magnetic field, eddy currents which will be established within the conductor will oppose the field. This opposition, in turn, will be reflected as a change in the impedance of the coil. The flow of eddy currents within the conductor is a function of such variables as electrical conductivity and permeability, size, and configuration of the conductor as well as the possible presence of discontinuities. Thus, each of these can have an effect on the impedance of the coil.

As used to measure the thickness of stainless steel clad on the UO_2-stainless steel dispersion core, both the thickness and conductivity of the clad and core have an effect on the impedance of the test coil. Figure 2 illustrates in a qualitative fashion the changes that occur. Position A represents the impedance value of the coil in air undisturbed by external effects. Position B is the impedance of the coil in intimate contact with an infinite thickness of base core material. (An infinite thickness is defined as that thickness beyond which slight dimensional increases will not be detectable as impedance changes in the coil.) The curve B-C is the locus of impedance values produced by inserting clad material of increasing thickness between the core and coil. Thus, position C represents the impedance for an infinite thickness of clad material.

Equipment and Materials

Commercial instrumentation is available which will generate the high-frequency electrical signal and detect variations associated with the impedance

---

[1]J. W. Allen, R. A. Nance, and R. B. Oliver, "Eddy-Current Measurement of Clad Thickness," Am. Soc. Testing Materials, Spec. Tech. Publ. No. 223, 201 (1958).

[2]R. C. McMaster (ed.), Nondestructive Testing Handbook, sec. 36, vol II, The Ronald Press Company, New York, 1959.

UNCLASSIFIED
ORNL-LR-DWG 59202

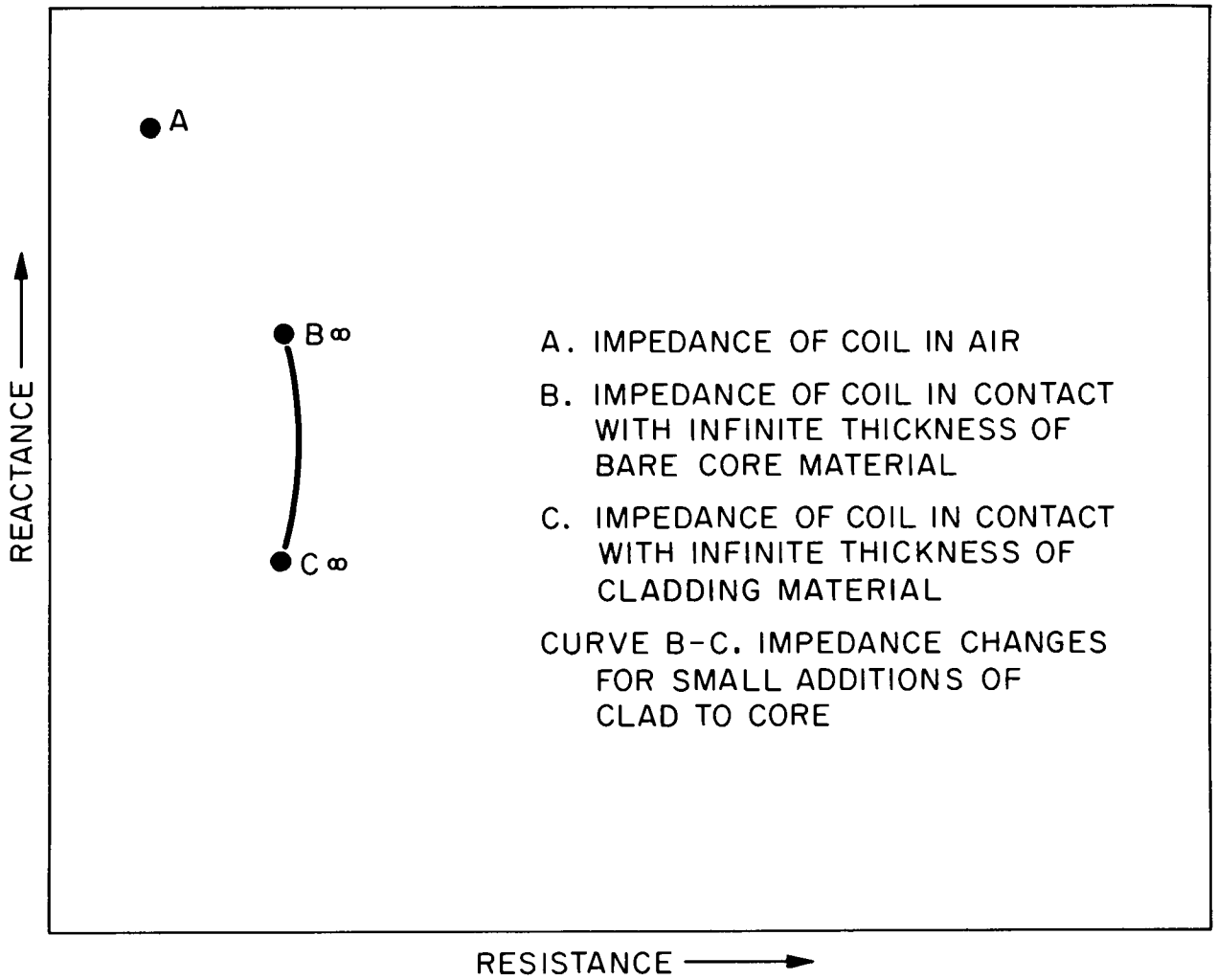

Fig. 2. Generalized Impedance Curve for Clad-Thickness Measurement.

changes in the probe coil. Two such devices were used in this phase of the study. One was the Radac Model 302 (The Budd Company Instrument Division, Phoenixville, Pennsylvania) and the other was the Dermitron (Unit Process Assemblies, Inc., New York City). Similar equipment from other manufacturers possibly would have served as well.

Reference standards of base core material and shims of type 347 stainless steel in varying thicknesses were manufactured for calibration purposes. Originally, the standard core material was a coined compact identical to the one used in the fuel plate fabrication. However, in this state, the densification and, consequently, the electrical conductivity are somewhat different from that of the core material in the finished rolled plate. For this reason, the calibrations did not adequately simulate the actual test conditions and were invalid. Proper core standards were obtained by milling the clad from one surface of a section of a fabricated fuel plate. The shims, to simulate varying thicknesses of cladding, received the same heat-treating schedule as the actual cladding. Using these materials, calibration curves such as seen in Fig. 3 were derived for instrument response versus shim (clad) thickness.

Test and Results

A number of measurements were made on fuel plates with unknown clad thickness using the calibration curves for each instrument to translate the response into a clad-thickness value. There was not precise agreement between the two instruments on some of the readings but this was not totally unexpected. The eddy-current frequency being used on each of the devices was considerably different (32 kc on the Radac and 256 kc on the Dermitron). The effective depth of penetration of the eddy currents is a function of the frequency with the lower frequencies being much more penetrating. Thus, the lower frequency would be more likely to be influenced by small variations in the core material which would be independent of clad-thickness changes. On the other hand, the higher frequency will be more influenced by small variations in the coil-to-specimen spacing which could cause a confusing change in the coil impedance and meter reading.

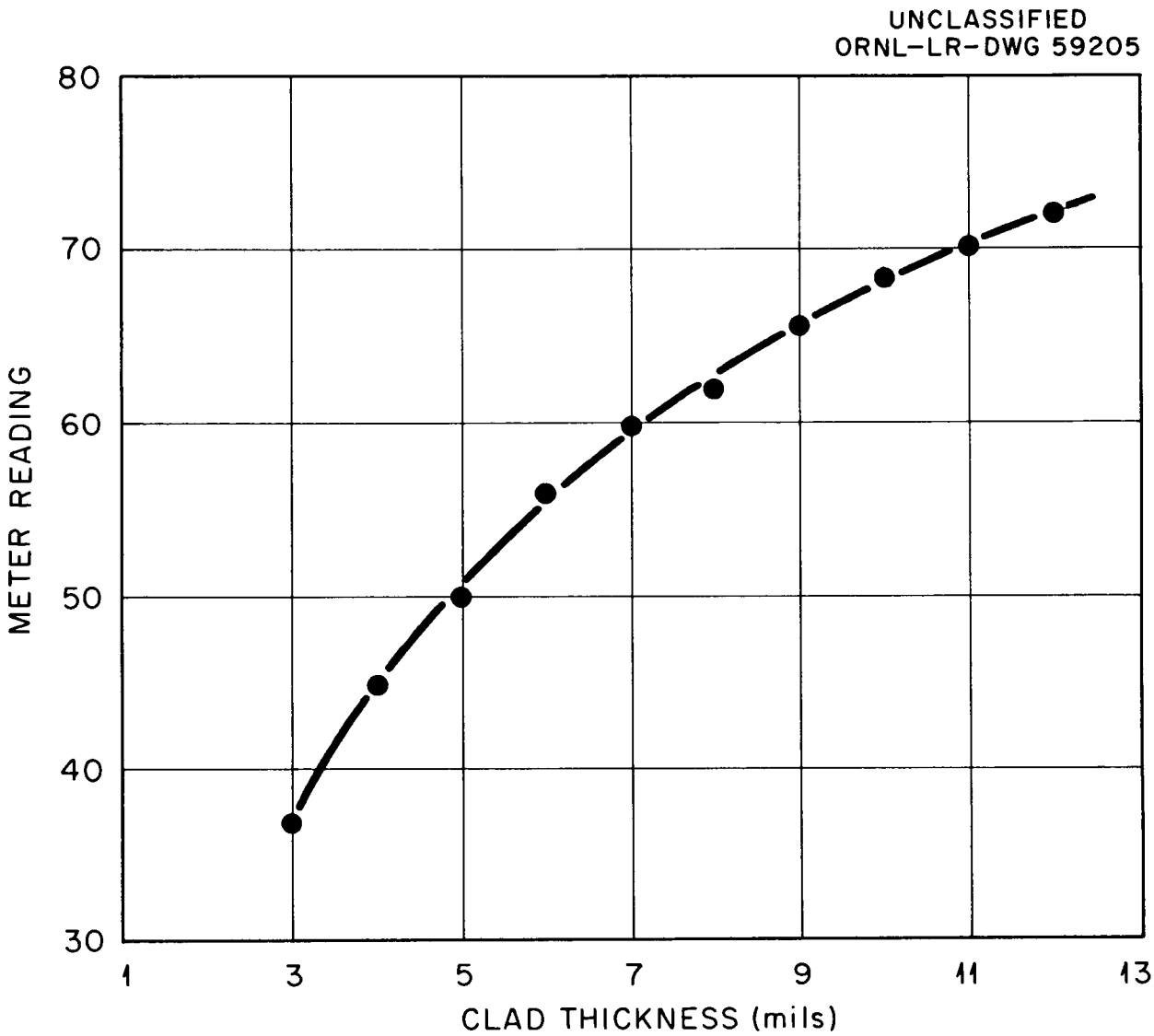

Fig. 3. Typical Calibration Curve for Eddy-Current Measurement of Clad Thickness.

Many of the measured specimens were then submitted to metallographic sectioning for optical measurements of the actual clad thickness. Figure 4 is a typical cross section of the clad and clad-to-core interface. The interface is almost indistinguishable, and the distance from the clad surface to the first UO_2 particle is quite variable. The eddy-current probe coils used are approx 1/4 in. in diameter, and the recorded response is an integrated effect of the area under the coil. Thus, it is apparent that a single optical measurement would be of little value in attempting to correlate or check the accuracy of the eddy-current measurement.

For this reason, two different metallographic sections were taken from the immediate area at which the clad thickness had been measured by the eddy-current technique. On each section, 10 random optical measurements were made across a span corresponding to the coil diameter, and an average clad-thickness value was obtained. The two sections from a single measured area provided further information on the localized average clad-thickness variations. Table 1 presents some typical data from both eddy-current and metallographic measurements. Comparison shows that the accuracy of the eddy-current test is at least ± 0.001 in. and in most instances considerably better.

Despite the fact that individual UO_2 particles penetrated closer to the surface than detected by eddy currents, a very good indication of the average clad thickness was obtained. With a proper appreciation of the limitations of this test system, it should be possible to provide valuable information and process control during fuel element fabrication and inspection.

ULTRASONIC DETECTION OF NONBOND AREAS

Purpose

A flaw or lack-of-bond condition at the core-clad interface of a fuel plate would impede the heat flow and produce a localized hot spot which could precipitate a failure of the element. Concern over this possibility has prompted the requirement for a nondestructive test to detect small areas of nonbond in fabricated fuel plates. This concern did not stem from any innate tendency for the

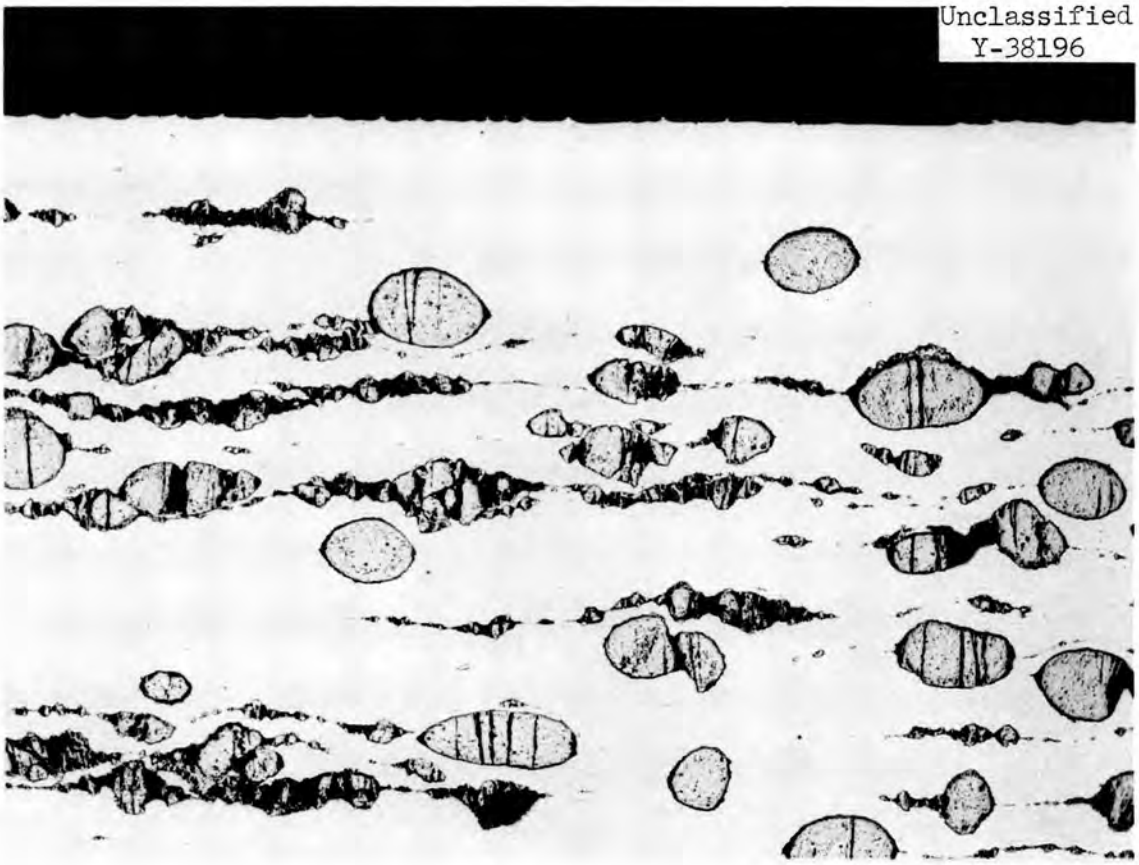

Fig. 4. Cross Section of Core-to-Clad Interface in Fermi Core. 100X.

Table 1. Comparison of Eddy-Current and Metallographic Measurements of Clad Thickness on the Fermi Core B Fuel Plate

Specimen Number	Eddy-Current Measurements		Metallographic Measurements	
	Radac (in.)	Dermitron (in.)	Section No. 1 (in.)	Section No. 2 (in.)
1	0.0051	0.0051	0.0045	0.0049
2	0.0063	0.0059	0.0053	0.0053
3	0.0037	0.0051	0.0041	0.0047
4	0.0045	0.0046	0.0040	0.0054
5	0.0041	0.0049	0.0038	0.0040
6	0.0037	0.0045	0.0046	0.0058
7	0.0054	0.0046	0.0050	0.0055
8	0.0054	0.0052	0.0044	0.0060
9	0.0056	0.0053	0.0048	0.0050
10	0.0056	0.0049	0.0045	0.0052

Core B materials combination to be susceptible to nonbond problems, but rather there was the realization that the elements would be operating under extreme service conditions.

Theory

Through-transmission ultrasonics[3] were selected as the best, readily available method for nonbond detection in the thin-clad plates. Although this method has been applied to the inspection of uranium or uranium alloy fuel plates, no information was available as to its suitability or attainable sensitivity when applied to a ceramic (UO_2) dispersion in stainless steel. The different acoustic properties of the dissimilar materials in the core and the possible localized inhomogeneities in the UO_2 concentration were expected to cause considerable difficulty in performing a sensitive inspection.

Figure 5 shows, in a schematic form, the test principles. A high-frequency ultrasonic beam is generated by a piezoelectric (or electrostrictive) transducer. This beam is transmitted through a coupling medium such as water. As the beam encounters an interface, a portion of the beam will be reflected, and a portion will be transmitted through the interface. The amount of reflection is dependent, in part, on the acoustic mismatch at the interface. Thus, a beam being transmitted from one transducer to a similar receiving transducer will be attenuated by the presence of intermediate interfaces and such other factors as scattering, absorption, divergence, etc. As long as the intermediate material is uniform, a constant signal amplitude will be detected by the receiving transducer. However, a localized condition of nonbond with its drastically different acoustical impedance will cause a reduction in transmission. The amount of reduction will be primarily a function of the nonbond area as compared to the cross-sectional area of the ultrasonic beam.

Equipment

Commercially available pulsed-ultrasonic instrumentation was used for this study. The principal component was the instrument that produced the electrical

[3]R. C. McMaster (ed.), Nondestructive Testing Handbook, sec. 43, vol II, The Ronald Press Company, New York, 1959.

UNCLASSIFIED
ORNL-LR-DWG 47489

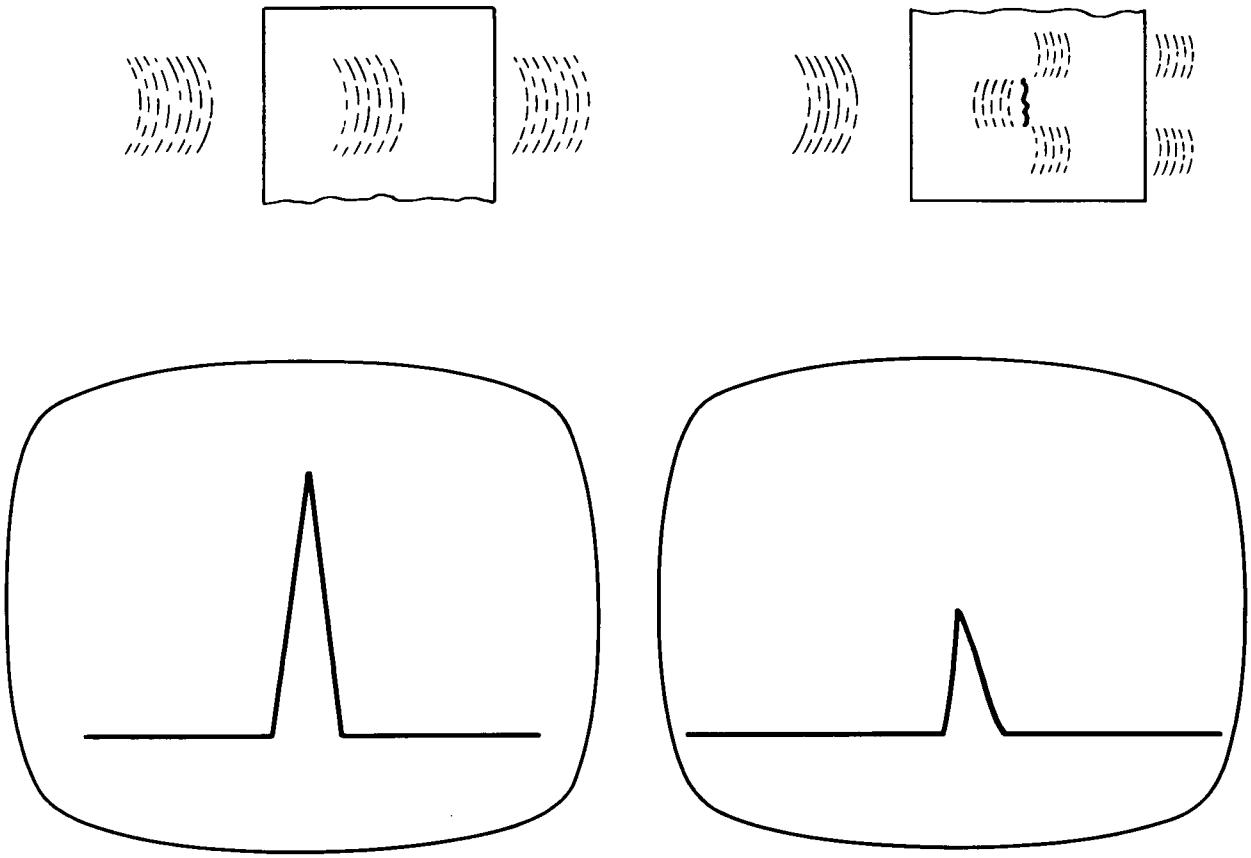

Fig. 5. Through-Transmission Ultrasonic Test Method.

signal to feed the piezoelectric transducer. This signal was a continuous series of 1-μsec pulses at a repetition rate of approx 600 pulses/sec. For rapid scanning over the plate surface, it is necessary to have the fast repetition rate to assure that every section of the plate which has been scanned has also been investigated by the ultrasound. Other features of the basic unit are detection, amplification, and display circuitry to process the data relative to the amount of sound transmitted through the fuel plates.

The basic instrument used was the Immerscope (manufactured by the Curtiss-Wright Corporation of Princeton, New Jersey). Other similar commercial instruments would possibly have served as well. An item of auxiliary instrumentation provided an electronic gate to select and process the transmitted pulse. This pulse subsequently operated visual and/or audible alarms and generated an output signal suitable for actuating the stylus of a plan-view recorder. Thus, a map of the plate and its nonbond area was provided as a permanent record.

Mechanical scanning equipment was required to provide precise control of the scanning parameters. Two different systems were used with reasonable success. The first consisted of a conventional ultrasonic tank equipped for motorized X-Y scanning with the search tube containing the transducer being mounted in a vertical position. Figure 6 illustrates the relative position of the transducer and inspected plate. Because of certain physical limitations in the search tube clamps and other mechanical features, it was necessary to use the reflector to relay the ultrasound to the detecting transducer. The fuel plate was in a fixed, horizontal position and the transducer array was moved along the plate to inspect a linear element. At the conclusion of each linear scan, a transverse motion and reversal permitted a parallel return scan. The amount of transverse motion, or indexing, was determined by a number of variables such as the size of the ultrasound beam, the amount of overlap desired or required, the size of nonbond being sought, and the instrument sensitivity. The information concerning X-Y mechanical motion was fed to the servo-driven electro-sensitive paper recorder by means of data potentiometers. A principal advantage of this system was the ready availability of the tank system complete with mechanical drive and data potentiometers. Some difficulties were encountered with instability of the search

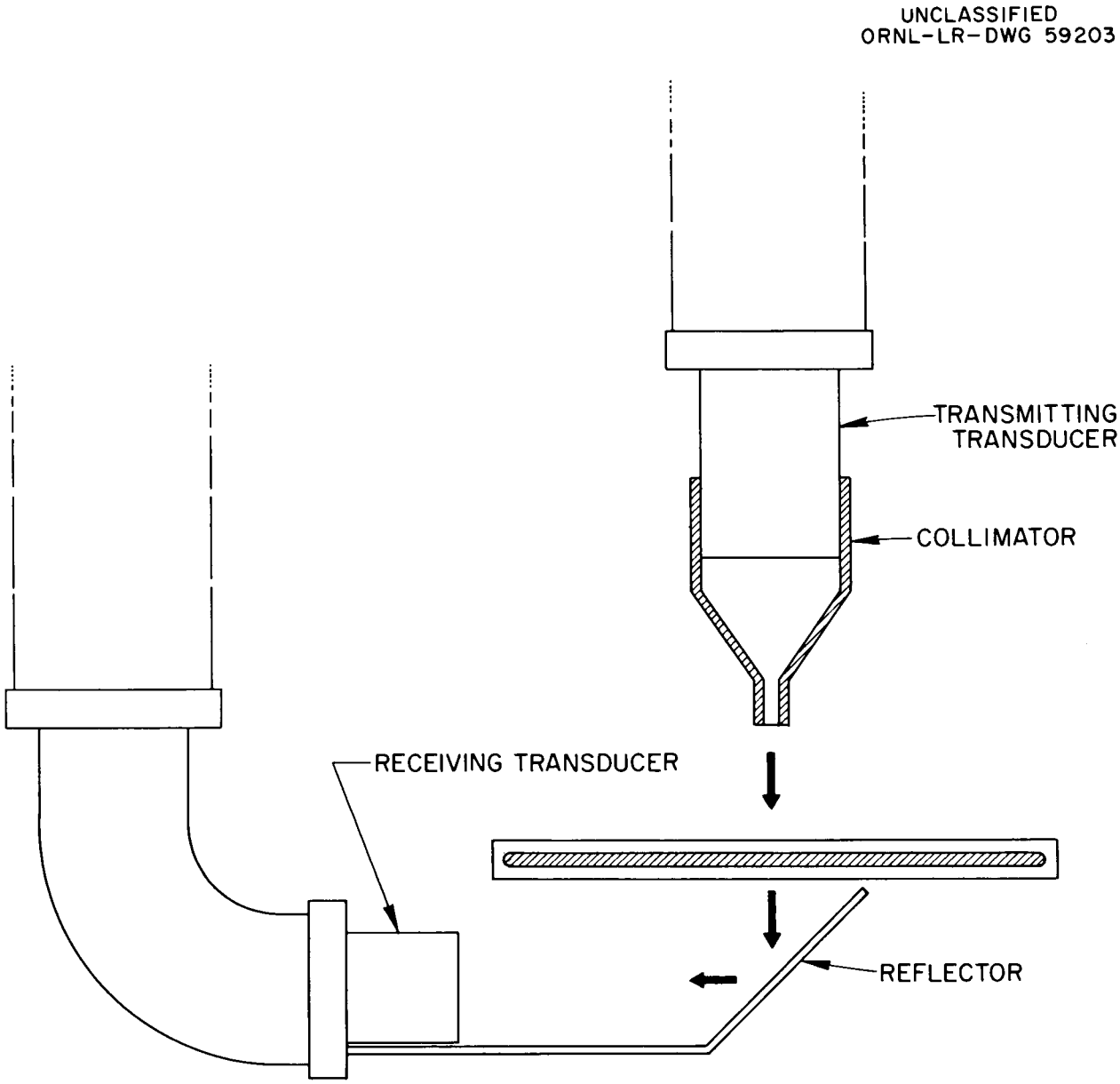

Fig. 6. Ultrasonic Scanning of Fuel Plate in Horizontal Plane.

tube alignment with the sharp reversals associated with rapid scanning. Another problem with this system was the catenary action with longer lengths of unsupported fuel plate in the horizontal position.

The other mechanical system which was temporarily employed held the fuel plate with the transverse direction (width) of the plate vertical. The plate itself was moved in a longitudinal direction to accomplish the linear scan, and the transducer system was adjusted in a vertical direction to accomplish the indexing. This system is shown in Fig. 7. The mechanical motion for the plate was achieved by means of a continuous roller-chain drive originally designed as part of a tank system for the inspection of tubing.[4] The transverse adjustment of the opposing transmitting and receiving transducers was accomplished with the cross-feed mechanism of a small lathe. As used during the feasibility study, manual operation of the cross-feed was necessary, but this can be readily mechanized. Data potentiometers were used to translate mechanical motion into a driving signal for the plan-view recorder. This seemed to be a more stable system than the one previously described, since the only motions encountered for both plates and search tubes are in their most rigid direction.

Longitudinal scanning speeds in excess of 200 in./min were readily attainable with either system. Faster scans would be practical if mechanical stability and the necessary instrument responses were maintained.

The first chart recordings were produced with a positive writing voltage on the stylus at all times if adequate transmission were available through the plate to present a signal of sufficient amplitude. Decreases in amplitude below a preset level (as would be caused by a nonbond) would reduce the writing voltage and the resultant was a map of the scanned element similar to that shown in Fig. 8. The white areas represent intentional nonbond conditions that have been fabricated in a sample fuel plate. Modification of the instrumentation allowed a writing voltage to be impressed upon the pen only during the presence of decreased amplitude which produced a recording such as is shown in Fig. 9. This greatly reduced pen wear problems and seemed to offer greater contrast and a readily interpretable recording.

---

[4]R. B. Oliver, R. W. McClung, and J. K. White, "Production Inspection of Pipe and Tubing by the Immersed Ultrasonic Method," Am. Soc. Testing Materials, Spec. Tech. Publ. No. 223, 62 (1958).

Unclassified
Photo 53422

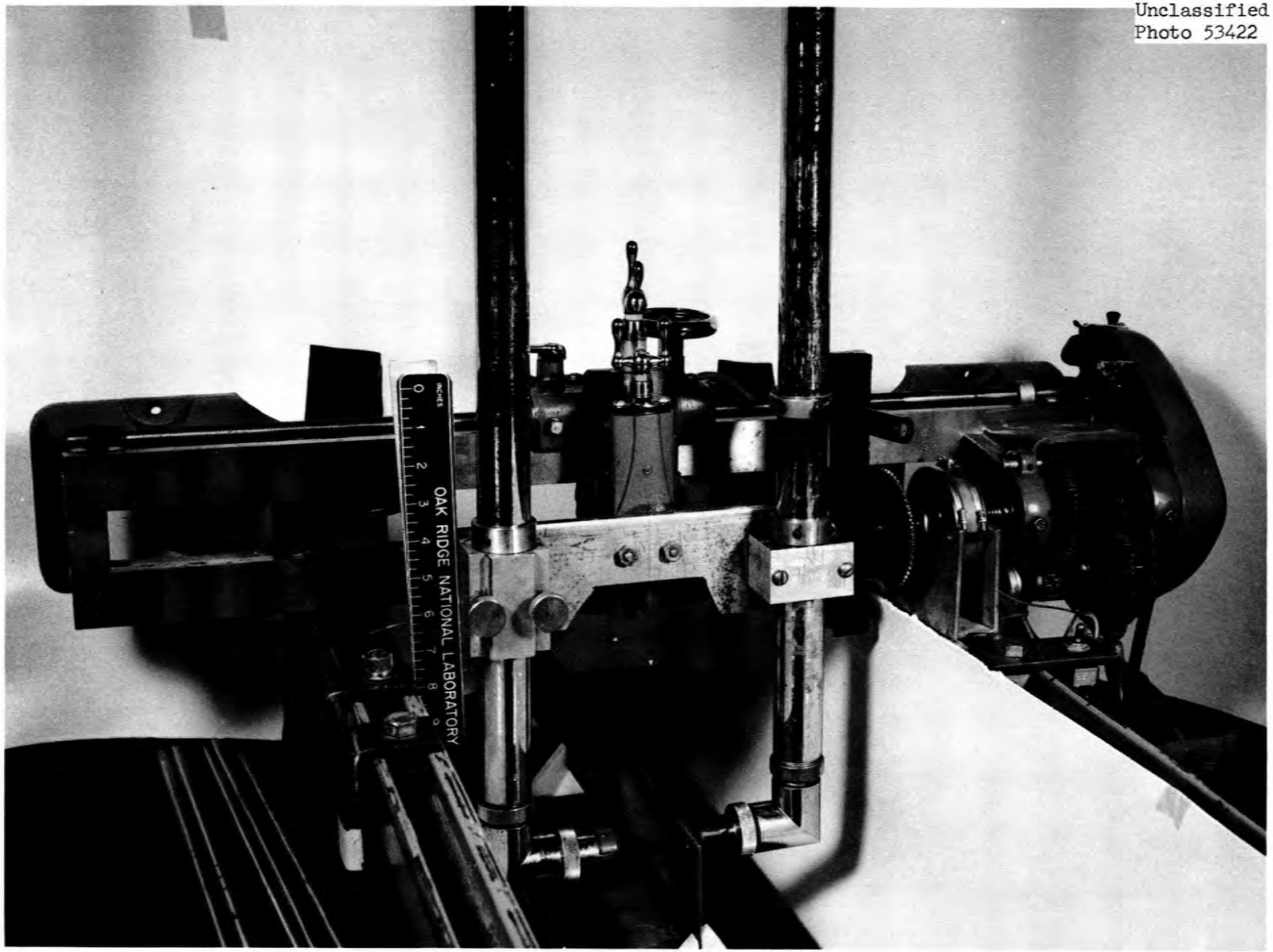

Fig. 7. Ultrasonic Scanning of Fuel Plate in Vertical Plane.

UNCLASSIFIED
ORNL-LR-DWG 59200

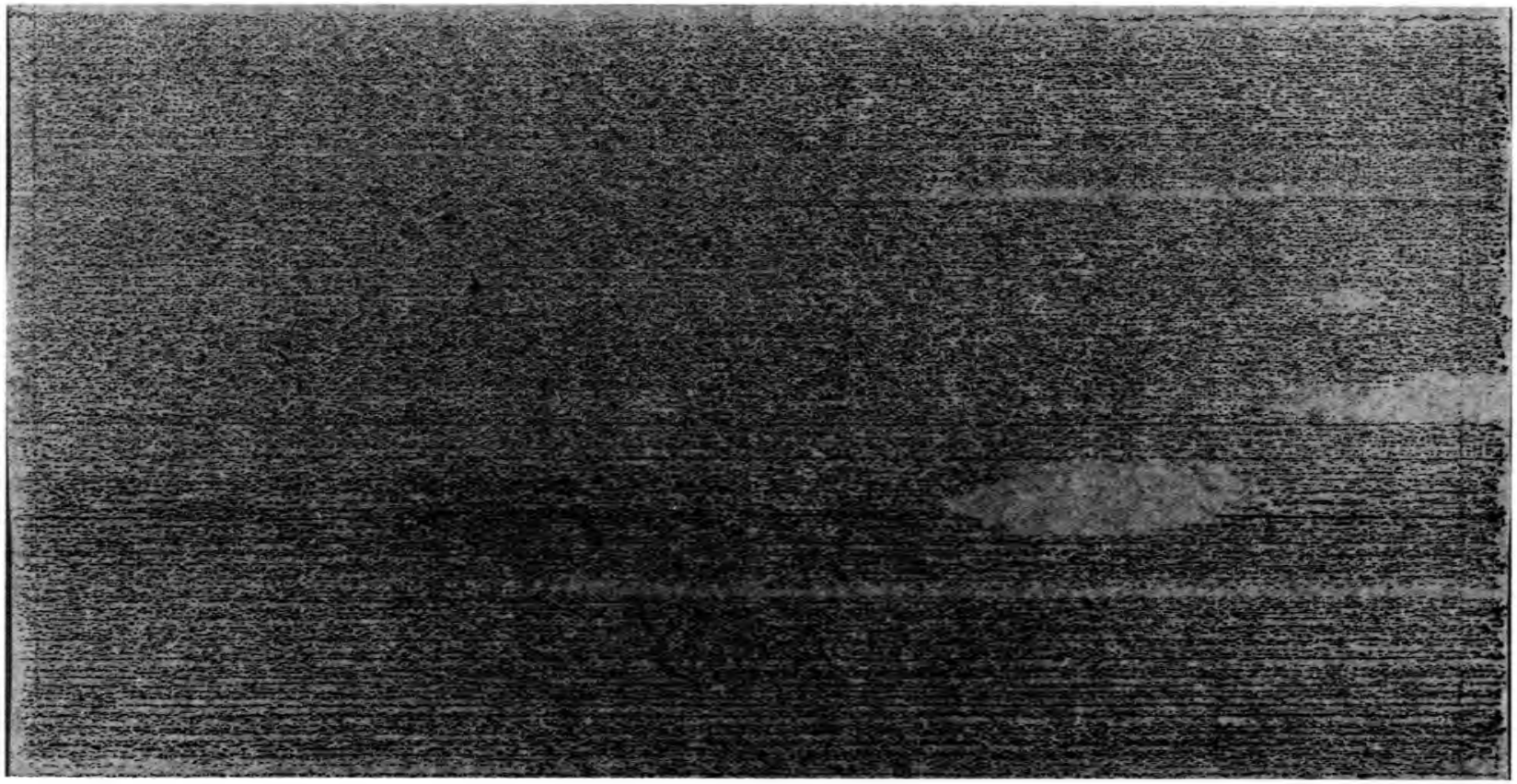

Fig. 8. Plan-View Record of Fuel Plate Ultrasonically Inspected for Nonbond. (The light area denotes nonbond.)

UNCLASSIFIED
ORNL-LR-DWG 59201

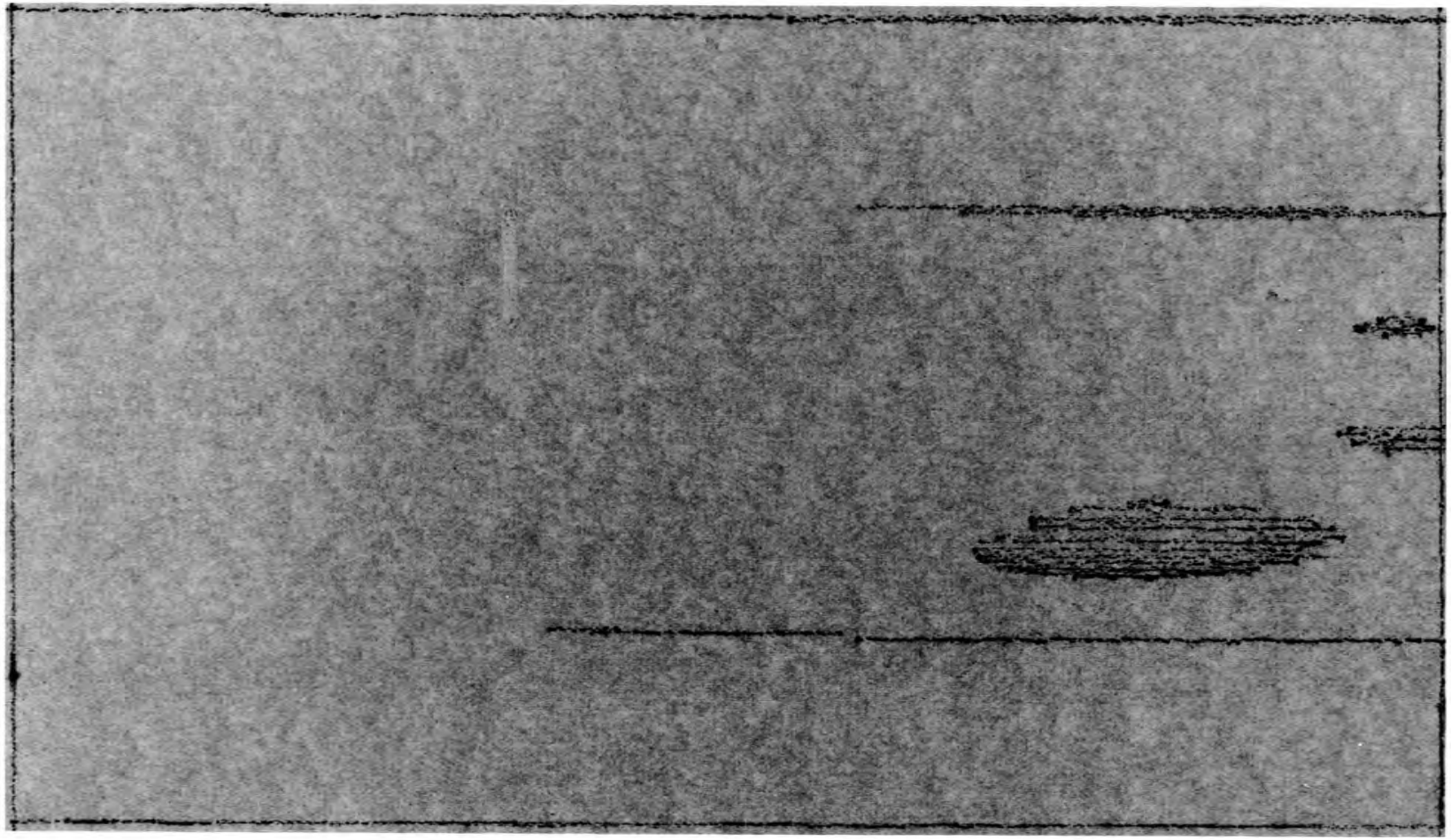

Fig. 9. Plan-View Record of Plate Shown in Fig. 8. (Use of revised instrumentation shows dark areas for nonbond.)

Reference Standards

Nonbond areas of known size in standard fuel plates were needed for instrument calibration, inspection standardization, and, more particularly in the early stage, for the determination of attainable sensitivities. Several different fabrication techniques were studied. One consisted of end milling shallow, flat-bottom holes of varying diameters in the initial core blank, filling these holes with Al_2O_3, and then rolling this blank into a conventional fuel plate configuration. There was considerable difficulty in obtaining nonbond areas of predetermined size, particularly of small areas, since a significant elongation of the simulated nonbond occurred in the rolling direction. On occasion, sufficient ultrasonic coupling existed through the tightly compacted Al_2O_3 after rolling to reduce the response relative to that obtained on a true nonbond of comparable size. Attempts to use small pieces of high-temperature mica to prevent bonding during fabrication were unfruitful due to the fracture and dispersion of the mica. The best and most reproducible fabrication technique involved the use of end mills to produce shallow, flat-bottom holes of known diameter in finished fuel plates. These holes were then plugged in such a fashion that the acoustic mismatch at the bottom of the hole corresponded as closely as possible to that expected from a naturally occurring nonbond. It was assumed that the nonbond would be an extremely thin void and would have a reflection coefficient $\left(\frac{\text{amplitude of reflected signal}}{\text{amplitude of incident signal}}\right)$ of 99% or greater. A rather quick method of obtaining this condition was to place a small thin piece of paper at the bottom of the hole. This paper was then covered as the hole was plugged with a water-proof substance such as wax or Apiezon (manufactured by Metropolitan-Vickers Electrical Company, Ltd.). Regardless of the plugging technique, care must be exercised to prevent improvement of the ultrasonic coupling across the interface at the bottom of the hole. Any such coupling will permit the transfer of energy which will reduce the response causing the reference defect to appear as a smaller nonbond area. This could obviously result in inspection at a greater sensitivity than is desired, producing spurious rejections.

Holes were drilled in both frame and core areas to varying depths to simulate nonbonds at the clad-to-core interface on either side of the plate

and possible discontinuities within the core itself. Because of the thin section of the test plate (approx 0.115 in.) relative to the distance between the transmitter and transducer (approx 2 in. in the vertical scanner) no significant difference was noted in the response for reference nonbonds of equal areas located at varying depths.

Test and Results

After some experimentation, 2.25 mc was chosen as the best available ultrasonic frequency for meaningful results. Higher frequencies would have been more susceptible to variations resulting from attenuation differences within the core and thickness changes in the fuel plate. Simulated nonbonds of 1/16-, 3/32-, and 1/8-in. diam with varying depths were placed in a sample test plate using the end-mill and plug technique. As mentioned previously, the response to a nonbond is detected as a decrease in transmitted sound and the degree of response is a function of the nonbond area as compared to the cross-sectional area of the sound beam. Since the most readily available transducers were 3/4-in. diam, reinforced-plastic collimators were used to restrict the sound beam and thus improve both sensitivity and resolution.

A number of prototype Core B fuel plates were examined using the reference plate as a standard. It was determined that the background variations in ultrasonic transmission due to the core quality were approximately equal to the response from a 1/16-in. nonbond, but less than that from a 3/32-in. nonbond. However, occasional variations associated with the UO_2 condition at the core edge (not nonbonds) produced signals comparable to the 3/32-in. nonbond, but smaller than the 1/8-in.-diam reference nonbond. Thus, if the core-edge condition is acceptable, the practical limit of testing will be for nonbonds comparable to the 1/8-in. standard. Using this level of sensitivity, it was determined that a 1/8-in.-diam aperture on the collimation was optimum. This in turn allowed an index of approx 1/16 in. between parallel scans to assure detection of rejectable nonbonds. Use of smaller apertures decreased the allowable index with associated increase in inspection time. Larger apertures permitted no significant increase in index size but sharply decreased the response to rejectable nonbonds.

Approximately 20 fuel plates were examined using this ultrasonic technique with a sensitivity capable of detecting 1/8-in.-diam nonbonds. No rejection was made. The confidence level in this inspection technique, however, was strongly established during the development and testing of the reference standards. For instance, although the use of Al_2O_3 was unsuccessful for fabrication of acceptable standards, it did provide some interesting results. Figure 10 is a drawing which shows a fuel plate containing purposely made nonbond areas which were detected by the ultrasonic test. As may be seen, a number of metallographic sections were taken through nonbond areas. Excellent correlation was obtained on defect size and position. The drawing in Fig. 11, for example, represents the metallographic cross section of defect No. 16 of Fig. 10. The actual nonbond area in the specimen was much thinner than is depicted in this illustration. It is evident that the nonbond size was accurately determined. The slight offset in location marking could have been caused during recording or marking of the plate section or during metallographic processing.

From the results of the ultrasonics studies, it appears that adequate inspection can be made for nonbonds with areas the equivalent of 1/8-in.-diam circles. With appropriate equipment and instrumentation, inspection can be rapid, reliable, and relatively inexpensive.

RADIOGRAPHIC DETERMINATION OF INHOMOGENEITIES IN UO_2 CONCENTRATION

Purpose

In the design of the Core B fuel assembly, considerable effort is being expended to assure a uniform removal of heat to prevent localized hot-spot conditions which could result in fuel element failure. Care must be taken, therefore, to assure that variations in loading of the UO_2 fuel within the stainless steel matrix are inconsequential and excessive localized heat generation will not occur. For this reason, studies were conducted to demonstrate the feasibility of nondestructively detecting excessive inhomogeneity in the fuel.

UNCLASSIFIED
ORNL-LR-DWG 49966

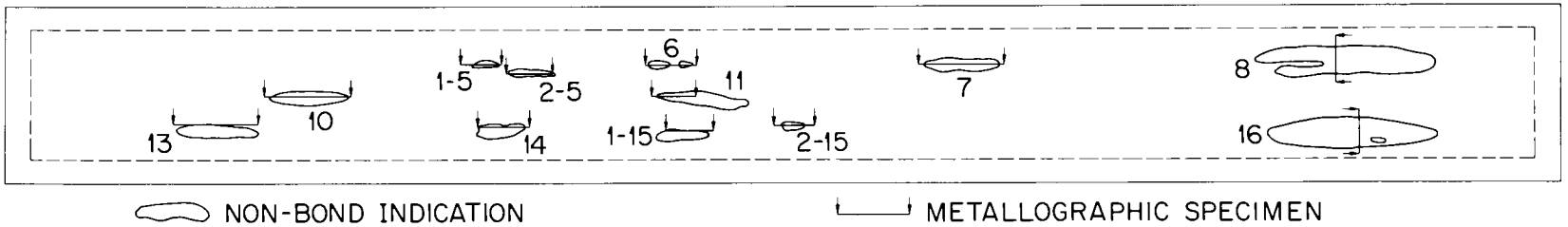

Fig. 10. Intentional Nonbond Areas Located by Ultrasonic Inspection.

UNCLASSIFIED
ORNL-LR-DWG 49965

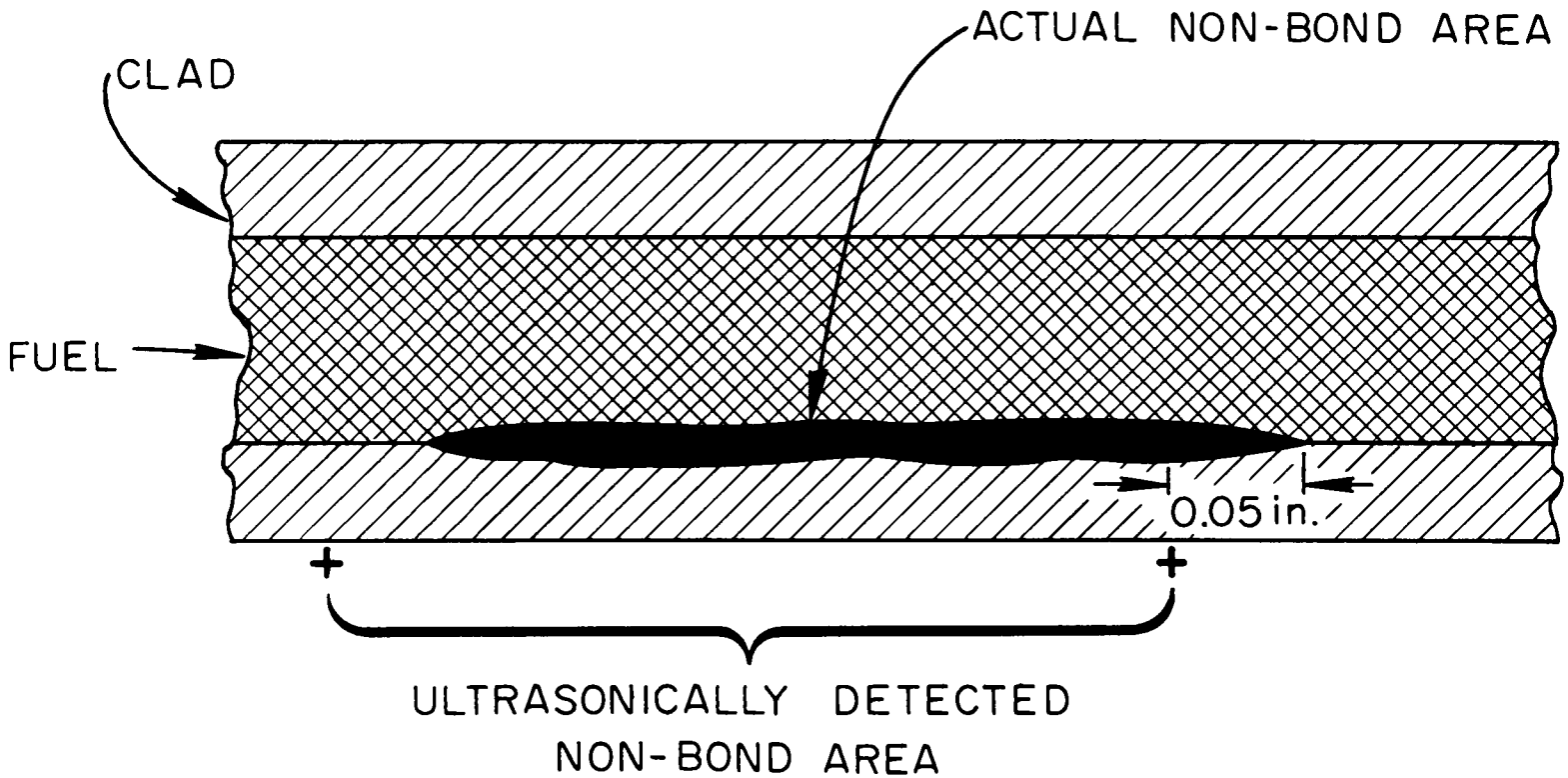

Fig. 11. Correlation Between Indicated and Actual Nonbond Areas.

Theory

A radiographic method was chosen to detect and measure the degree of fissile-compound variation within the fuel plates. It was recognized that other penetrating radiation techniques such as autoradiography or gamma-scintillation spectrometry could possibly be used for this problem with varying degrees of acceptability. It was felt, however, that the general availability of conventional x-ray equipment to most manufacturers made radiography an attractive approach. The radiographic technique, of course, produces a shadowgraph of film blackening on radiation-sensitive film according to the amount of radiation incident on the film. As x radiation passes through a specimen, it will be attenuated according to the section thickness and the absorption coefficient which increases with the atomic number or "Z" of the material. The thickness of the Core B fuel plate is nominally constant. The fabrication specifications, however, allow a tolerance on the UO_2 homogeneity of ± 5% from the nominal concentration. With such a solid fuel plate, it is apparent that any variation in UO_2 concentration will be accompanied by an offsetting change in the concentration of the stainless steel matrix to maintain constant volume conditions. However, since UO_2 has a much higher effective "Z" than the steel, there will be an x-ray intensity change directly related to UO_2 concentration.

Equipment

The industrial radiographic equipment which was available in the Nondestructive Test Development Group laboratory was the Norelco MG-300 unit manufactured and sold by Philips Electronic Instruments of Mount Vernon, New York. The x-ray tube which was used has a 5-mm focal spot. Conventional cassette holders were used with type "M" Eastman Kodak film. This fine-grained film was chosen to attain maximum contrast. Similar results would be expected with other brands of high-contrast fine-grained film.

Reference Standards

In common with most other nondestructive tests, the radiographic procedure requires special standards to calibrate and establish the technique. As a matter of fact, most of the work accomplished in this phase of the feasibility study was directed toward the establishment and use of adequate standards. As was mentioned previously, the tentative procurement specification allowed a tolerance on the UO_2 concentration of ± 5% from nominal. A series of UO_2-stainless steel samples were pressed and sintered to cover a wide range of UO_2 concentrations. The samples were made in two parts — a few thick sections with 25 vol % UO_2 in stainless steel, and several thinner sections with varying UO_2 volume concentrations. The combination of one thick and one thin sample would then have the equivalent thickness of a fuel plate, and varying UO_2 concentrations could be established for radiography. During fabrication, some difficulty was encountered in obtaining uniform material densities from sample to sample. Further, in these pressed and sintered samples, it was not possible to attain the high density (94% of theoretical) which was regularly measured in hot-rolled fuel plate cores. For these reasons, several calculations were made and correction factors applied to simulate as nearly as possible an actual fuel element.

Since x-ray attenuation in a material is normally affected in accordance with the product of density $\left(\frac{g}{cm^3}\right)$ x thickness (cm) and the plate has a constant thickness, all of the calculations have been made for UO_2 and stainless steel quantities in terms of the units, g/cm^2. Appendix A presents the details of the simple assumptions and calculations which were made for the combination of one thick and one thin standard sample to simulate a fuel plate section with a known UO_2 concentration in g/cm^2. As may be seen from the calculations, it was necessary to add shims of stainless steel to bring the corrected thickness up to that of the nominal 0.115-in.-thick fuel plate. The necessary corrections were made to each of the standards, and radiographs were made of the entire range of concentrations.

Tests and Results

The radiographs were taken at 72-in. focus-to-film distance. This large distance provided a very uniform radiation intensity over an area which could accommodate several of the Core B plates. A series of exposures at varying x-ray energies demonstrated that a value of 130 kvcp would provide the maximum radiographic contrast on the film for a constant variation in UO_2 loading. Film densities in the range of 2.0 to 2.5 seemed to be optimum. The film was processed in accordance with standard commercial practice with eight minutes developing time. The density of the dry processed film was then measured by the through-transmission method using the MacBeth-Ansco Model 12A Densitometer (manufactured by the MacBeth Instrument Corporation of Newburgh, New York).

The curve in Fig. 12 is a plot of grams of UO_2 per square centimeter versus the film density through the region of interest. It is obvious that an adequate density difference can be attained permitting ready detection of the maximum and minimum allowable fuel loadings. It is anticipated that the production standards would simulate only the maximum and minimum conditions as go-no-go standards. There should be no real need for fuel concentrations other than these. Of course, these standards should reflect both the fuel plate-thickness tolerance of ± 0.001 in. and the UO_2 concentration tolerance, i.e., the maximum x-ray attentuation standard should represent an 0.116-in.-thick plate with the maximum allowable fuel concentration. Conversely, the minimum standard should represent an 0.114-in.-thick plate with the minimum fuel concentration. Appendix B illustrates the calculations by which the standard requirements may be determined.

It is recognized that minor variations in film exposure and processing will cause small changes in the attained film density for any constant absorption. Therefore, no absolute values of film density can be assigned any given UO_2 concentration. However, if such standards are radiographed simultaneously on the same film with the fuel plates, the exposure and processing variables will affect both standards and plates. Thus, direct comparison may be made for determination of the unknown UO_2 concentration.

Other reference standard fabrication methods have been attempted and demonstrated to be feasible. Figure 13 illustrates two such samples. The first is

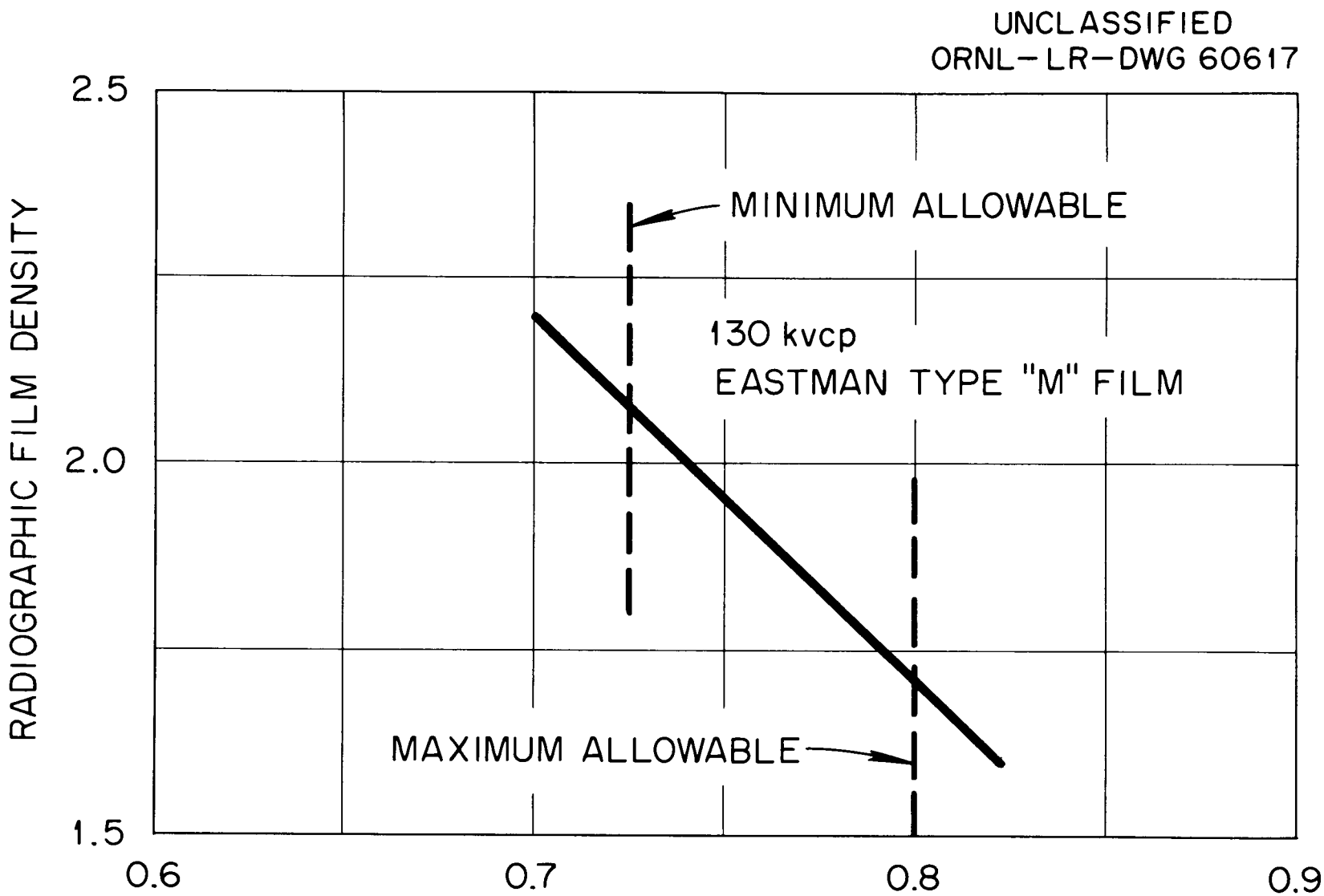

Fig. 12. Graph of Film Density versus UO_2 Concentration for Radiography of Fuel Plate.

UNCLASSIFIED
ORNL-LR-DWG 59204

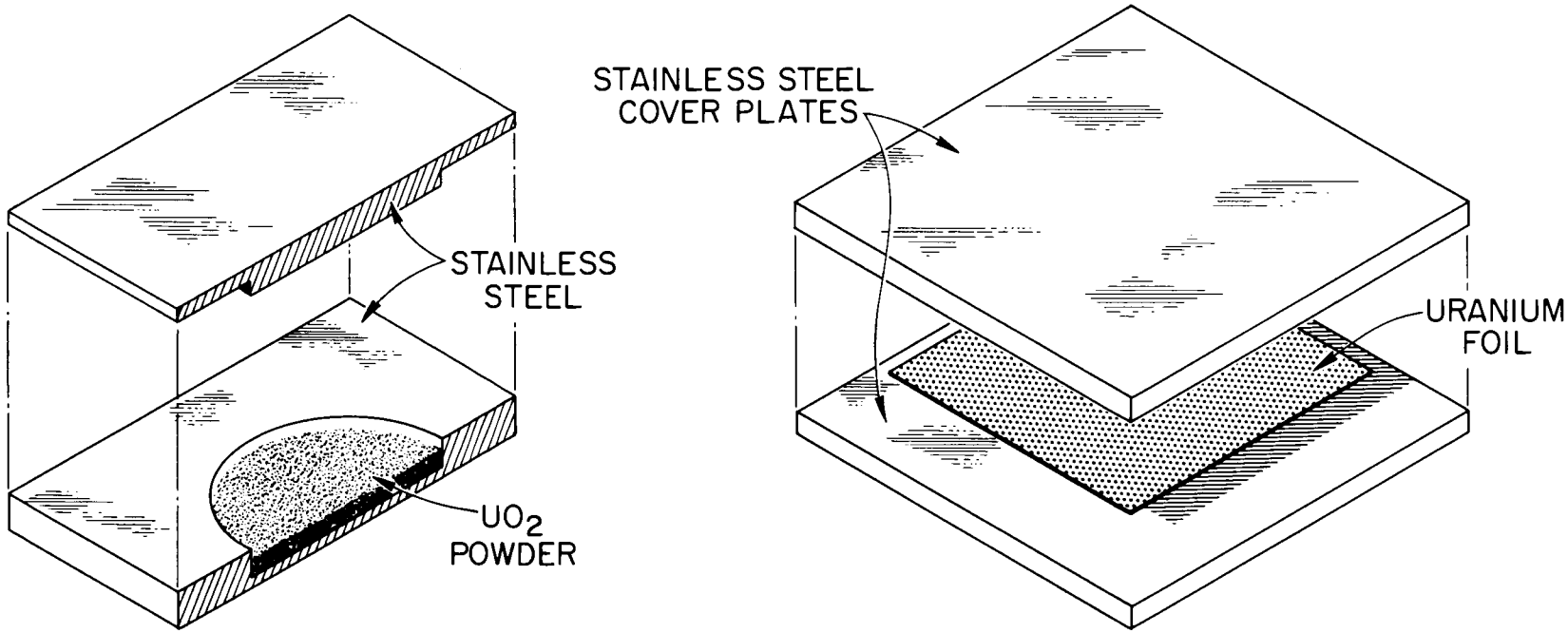

Fig. 13. Alternate Radiographic Standards for Core Homogeneity.

essentially a shallow, covered stainless steel cup containing the proper amount of UO_2 powder. The maximum and minimum amounts of UO_2 are the same as those calculated in Appendix B, i.e., 0.800 $\frac{g}{cm^2}$ and 0.724 $\frac{g}{cm^2}$, respectively. The necessary combined thickness of the top and bottom of the stainless steel container can be calculated in a similar fashion to that used in Appendix B. The exception, of course, is that all of the steel will be 100% of theoretical density rather than a portion being only 94.4% of theoretical density. The results of such calculations indicate that the required combined thickness would be 0.0819 and 0.0815 in. of stainless steel for the minimum and maximum tolerance conditions, respectively. Since a stainless steel-thickness change less than 0.001 in. will probably not be detectable when radiographed with the UO_2, these thickness values could be adjusted to 0.082 in. for both the maximum and minimum conditions.

The second standard in the illustration is a sandwich construction of uranium foil between stainless steel cover plates. The total stainless steel thickness is the same (0.082 in.) as was calculated for the previous standard. The uranium content of the UO_2 is assumed to be 88% and the density of uranium is 18.68 g/cm^3. These quantities combined with the calculated maximum and minimum UO_2 concentrations dictate uranium foil thicknesses of 0.01489 and 0.01344 in. This type of sample, of course, ignores the contribution of the oxygen in the UO_2 to the total radiation absorption. However, using theoretical mass absorption coefficients,[5] it can be shown that the change in absorption due to this assumption is 1% or less. It is felt, therefore, that the small difference may be more than offset by the greater ease of standard fabrication. The principal problem with this type standard is the visual appearance of the radiograph with the foil standard having a uniform tone as contrasted to the "salt-and-pepper" effect of the dispersion core.

Test samples of each of these reference standard concepts have been fabricated and radiographed. The results as determined by film densitometry indicate that each would be a reasonable and acceptable standard. A further conclusion

---

[5]E. Storm, E. Gilbert, and H. Israel, Gamma Ray Absorption Coefficients for Elements 1 Through 100 Derived from the Theoretical Values of the National Bureau of Standards, LA-2237 (Nov. 18, 1958).

is that the radiographic and densitometric system should provide an adequate test for core homogeneity. Regardless of the standard fabrication procedure, the accuracy of a standard should be established by comparison with analytical chemistry data on fabricated fuel plates.

Special Note on Duplicate Radiography

It has been the practice[6] to radiograph all test plates to determine the core shape and location relative to the stainless steel frame as a guide for machining. Of course, this requires low-density radiographs to prevent over-exposure of the frame area. However, it was demonstrated that a single x-ray exposure with duplicate films is sufficient to provide radiographs for both core homogeneity and location information. The film nearest the test piece is normally exposed to an approx 2.0 density for the homogeneity study. An 0.010-in.-lead filter placed in front of the second film will reduce the exposure such that adequate core location measurements can be made.

COOLANT CHANNEL SPACING MEASUREMENTS

Purpose

The Fermi reactor was designed primarily to produce large quantities of thermal energy at very high power densities. The extraction of this heat requires coolant channels interspersed between each fuel plate as shown in Fig. 14. A constant flow of sodium through the reactor core maintains a dynamic balance of heat production and removal. It is evident that too little coolant flow could cause temperatures in excess of the tolerance of the fuel and structural materials, and failure could occur. Nonuniform channel spacings could also produce asymmetrical temperature distributions and high thermal stresses. For these reasons, rigid requirements have been established on

---

[6] J. H. Cherubini, R. J. Beaver, and C. F. Leitten, Jr., Fabrication Development of UO_2-Stainless Steel Composite Fuel Plates for Core B of the Enrico Fermi Fast Breeder Reactor, ORNL-3077, p 46 (April 4, 1961).

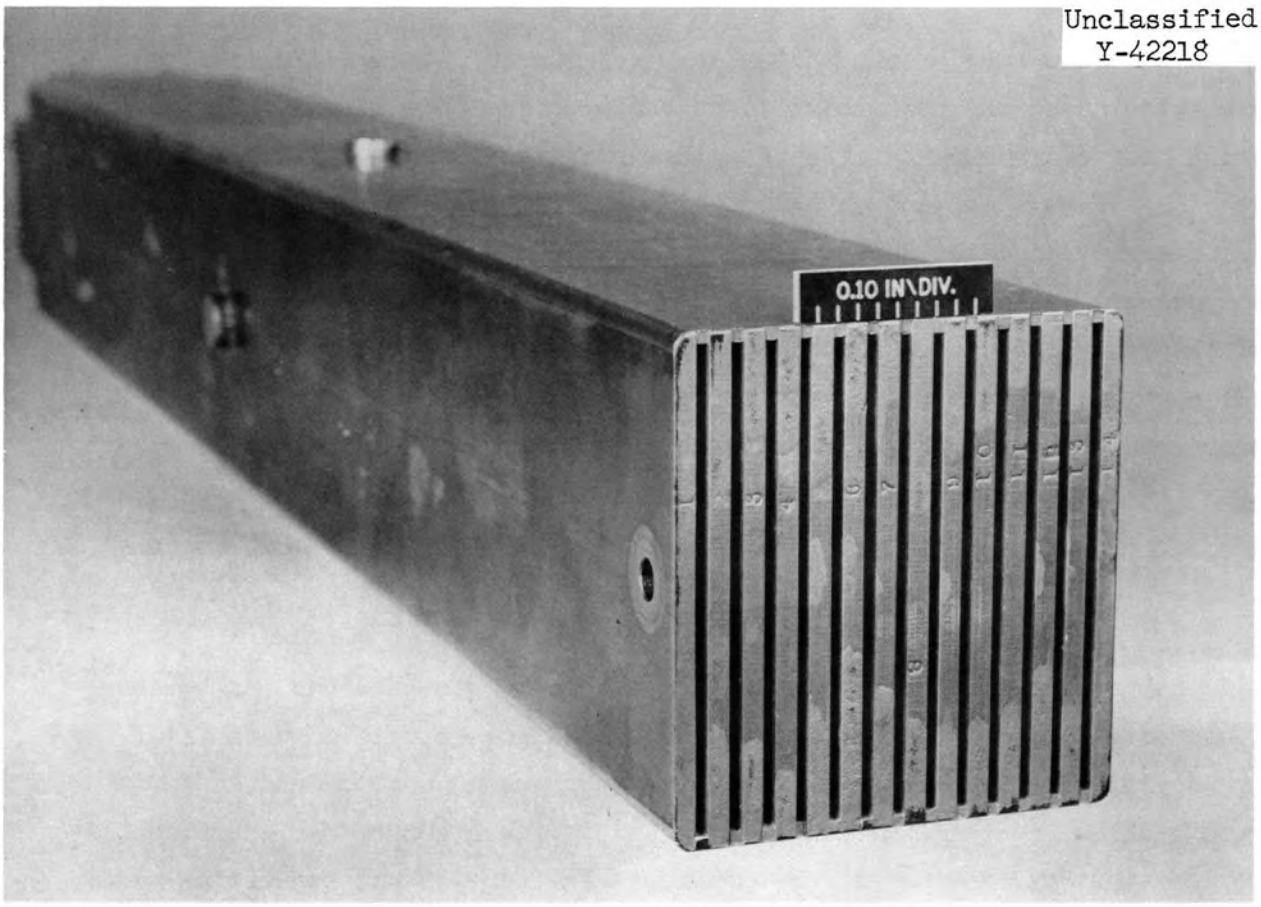

Fig. 14. Coolant Channels Between Fuel Plates.

coolant channel dimensions and tolerances. This, in turn, presents a need for an accurate measuring system to assure that the prescribed limits have been met. The specified spacing between respective fuel plates has been established as 0.054 in. with a nominal tolerance of ± 0.002 in.

Theory

As in the case of clad-thickness measurements, the eddy-current method[7] was selected as the best solution to the problem. One of the variables to which most eddy-current techniques is sensitive is that of the coil-to-specimen spacing. Figure 15 is a normalized impedance plane plot which demonstrates in a qualitative fashion the impedance changes for a test coil as a function of varying conductivity, frequency, and coil-to-metal spacing or "lift-off." This "lift-off" effect is utilized in the measuring of the coolant channel spacing. Relatively high frequencies (in the megacycle range) are preferred for the best accuracy since this produces the greatest response for a small movement near the eddy-current coil.

Equipment

Commercial instrumentation was available to generate the appropriate frequencies and to indicate the impedance changes associated with "lift-off" or spacing variations. Among the instruments which have been used for this type problem are the Laminagage (licensed for manufacture by General Motors Corporation) and the Dermitron (manufactured by Unit Process Assemblies of New York, New York). Special test probes for indirect measurements were designed and developed for this unique application. Figure 16 is a drawing showing the probe head used to make the desired measurement. The eddy-current coil is affixed to a long, slender tape which is used as the extension mandrel to insert the coil into the desired position. The ferromagnetic leaf spring

---

[7]C. V. Dodd and R. W. McClung, "Fuel Element Coolant Channel and Other Spacing Measurements by Eddy-Current Techniques," Paper presented at the Annual Meeting of the American Nuclear Society, Pittsburgh, Pa., June 7, 1961.

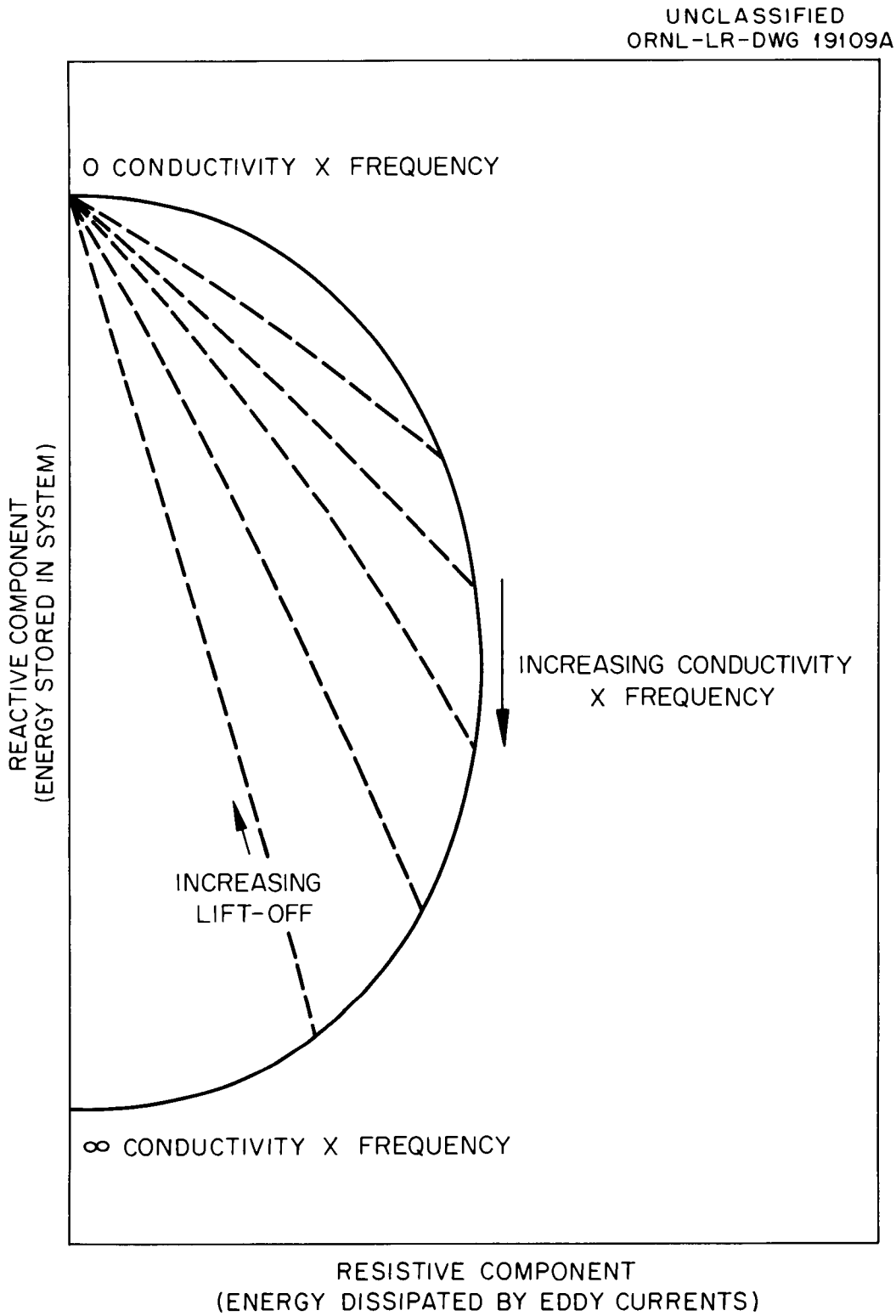

Fig. 15. Diagram to Illustrate the Impedance Changes Due to Coil-to-Specimen Spacing Variations.

UNCLASSIFIED
ORNL-LR-DWG 50492

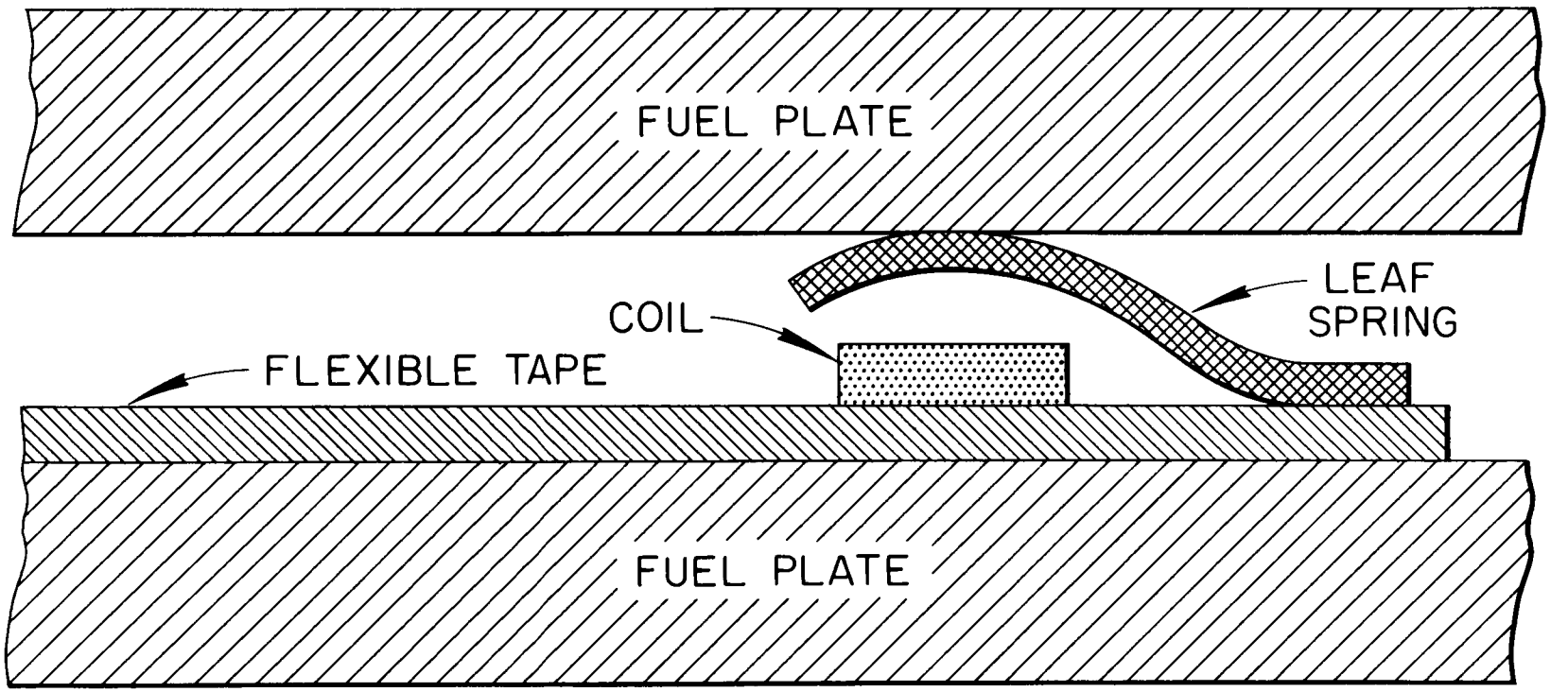

Fig. 16. Eddy-Current Probe Head for Coolant Channel Spacing Measurements.

which is mounted over the coil presses against the opposing fuel plate. Thus, as the fuel plate spacing varies, the leaf spring will move closer to or farther from the coil. The resultant impedance changes due to coil-to-spring variations can be calibrated in terms of space dimensions. The frequency of the eddy-current signal and the thickness and permeability of the leaf spring prevent unwanted signals due to variations in the fuel plate itself.

Tests and Results

Calibration standards were produced to span the measuring range with the desired intermediate dimensions. The standards consisted of a clamped assembly of small, flat parallel plates separated by gage blocks. This provided a known, accurate space for probe insertion and subsequent instrument calibration. To avoid conversion problems, a special direct-reading meter scale was made. In Fig. 17, a typical scale may be seen attached to the eddy-current instrument. The prototype probe is in the foreground. Calibration accuracies with this system for the required 0.050- to 0.060-in. span are 0.0005 in. This device has been in use through the major portion of the element fabrication development and a very large number of measurements have been taken. The reproducibility of repeated measurements is 0.0005 in. For production inspection of this and similar elements, the technique would be very amenable to mechanization and recording or complete automation.

SUMMARY

The cited investigations have determined the feasibility of a number of nondestructive evaluations proposed for the Core B fuel element of the Enrico Fermi Fast Breeder Reactor. It has been demonstrated that an eddy-current technique can be used to measure the average fuel plate clad thickness with an accuracy of ± 0.001 in. or better. With a proper appreciation of the limitations of the test system, it will give assurance that the specified cladding is present on the finished fuel plates.

The through-transmission ultrasonic technique can readily detect areas of nonbond 1/8 in. in diameter between the core and clad. With appropriate

Unclassified
Photo 52480

Fig. 17. Calibrated Scale for Eddy-Current Spacing Measurements.

electronic and mechanical features, a rapid reliable test system is possible for the complete inspection of fuel plates for bond integrity.

Radiography and film densitometry will be an adequate tool for the detection and measurement of excessive inhomogeneities of the UO_2 distribution within fuel plates. Proper fabrication and application of the reference standards will provide a direct representation of the specified limits of UO_2 concentration.

An eddy-current technique which has been used throughout the fuel element fabrication program will measure the coolant channel spacing between adjacent fuel plates with an accuracy of ± 0.0005 in. This rapid, accurate, and economical measuring system can be readily mechanized and automated for production-line operation.

The proper application of each of these tests should provide valuable information for process control during fuel element fabrication and give assurance that the completed fuel elements conform to the particular requirements of the procurement specifications.

ACKNOWLEDGMENTS

The author wishes to acknowledge the early work on clad-thickness measurements performed by R. A. Nance, formerly with the Nondestructive Test Development Group. Further recognition is given to A. L. Lotts of the Powder Metallurgy Group and J. H. Cherubini of the Fuel Fabrication Group for their work in the fabrication of standards; and to W. C. Thurber of the Reactor Projects Section for his coordination efforts.

APPENDIX A

Calculations for Correction Factors on UO_2-Stainless Steel Radiographic Reference Standards

A. Assumptions

1. The fuel plate will be 0.115 in. thick.
2. The core dimensions will be 18 in. (45.7 cm) long x 2.18 in. (5.54 cm) wide.
3. Clad thickness will be 0.005 in. ± 0.001 in.
   (The above values are nominal from preliminary procurement specifications.)
4. The fabricated fuel plate density will be 94.4% of theoretical (observed through actual plate fabrication).[8]

B. Thick Samples (All had same nominal concentration.)

1. Original charged weight

   14.198 g UO_2
   22.082 g Type 347 stainless steel (SS)
   36.280 g Total

   $$\frac{14.198}{36.280} = 0.3913 \text{ wt fraction of } UO_2$$

   $$\frac{22.082}{36.280} = 0.6087 \text{ wt fraction of SS}$$

2. Sample density = $7.04 \frac{g}{cm^3}$ (measured)
3. Sample thickness = 0.179 cm (measured)
4. Concentration

   $$7.04 \frac{g}{cm^3} \times 0.179 \text{ cm} \times 0.3913 \text{ (wt fraction)} = 0.4934 \frac{g\ UO_2}{cm^2}$$

   $$7.04 \times 0.179 \times 0.6087 = 0.7676 \frac{g\ SS}{cm^2}$$

C. Thin Samples (Since these had varying concentrations of UO_2, only a typical calculation is presented.)

---

[8] J. H. Cherubini, R. J. Beaver, and C. F. Leitten, Jr., Fabrication Development of UO_2-Stainless Steel Composite Fuel Plates for Core B of the Enrico Fermi Fast Breeder Reactor, ORNL-3077, p 45 (April 4, 1961).

1. Original charged weight

$$\begin{array}{ll} 5.306 \text{ g} & UO_2 \\ \underline{11.536} \text{ g} & \text{Type 347 SS} \\ 16.842 \text{ g} & \text{Total} \end{array}$$

$$\frac{5.306}{16.843} = 0.3150 \text{ wt fraction of } UO_2$$

$$\frac{11.536}{16.842} = 0.6850 \text{ wt fraction of SS}$$

2. Sample density = $7.61 \frac{g}{cm^3}$ (measured)

3. Sample thickness = 0.1225 cm (measured)

4. Concentration

$$7.61 \frac{g}{cm^3} \times 0.1225 \text{ cm} \times 0.3150 = 0.2936 \frac{g\ UO_2}{cm^2}$$

$$7.61 \times 0.1225 \times 0.6850 = 0.638 \frac{g\ SS}{cm^2}$$

D. Combination of Thick and Thin Samples

1. For UO_2:

$$\begin{array}{ll} 0.4934 \frac{g\ UO_2}{cm^2} & \text{(thick sample)} \\ \underline{0.2936 \frac{g\ UO_2}{cm^2}} & \text{(thin sample)} \\ 0.7870 \frac{g\ UO_2}{cm^2} & \text{combination} \end{array}$$

2. For stainless steel:

$$\begin{array}{ll} 0.7676 \frac{g\ SS}{cm^2} & \text{(thick sample)} \\ \underline{0.6380 \frac{g\ SS}{cm^2}} & \text{(thin sample)} \\ 1.4056 \frac{g\ SS}{cm^2} & \text{combination} \end{array}$$

E. Determination of Equivalent Thickness of Combined Samples Assuming 94.4% of Theoretical Density

$10.96 \frac{g}{cm^3}$ (UO_2 density) x 0.944% of theoretical = $10.35 \frac{g}{cm^3}$ (UO_2 density in fuel plate)

$7.93 \frac{g}{cm^3}$ (SS density) x 0.944 = $7.49 \frac{g}{cm^3}$ (SS density in fuel plate)

$0.7870 \frac{g\ UO_2}{cm^2} \div 10.35 \frac{g}{cm^3} \div 2.54 \frac{cm}{in.} = 0.0299$ in. (effective UO_2 thickness)

$1.4056 \frac{g\ SS}{cm^2} \div 7.49 \frac{g}{cm^3} \div 2.54 \frac{cm}{in.} = \underline{0.0739}$ in. (effective SS thickness)

0.1038 in. combined thickness

F. Correction to Nominal Core Thickness

0.1038 in. is 0.0012 in. or 1.2 mils thinner than the nominal 0.105-in.-thick core (nominal plate thickness less 2 times the clad thickness).

This may be added as stainless steel shim. Correction may be needed for using 100% dense shim stock to "make up" for 94.4% dense core material.

0.0012 in. needed x 0.944 = 0.0011 in. of stainless steel shim needed.[9]

G. Total Plate Thickness

The 0.0011-in. correction and the 0.010-in. nominal clad thickness added to this standard sample combination will result in the equivalent nominal plate thickness of 0.115 in. with a core density of 94.4% of theoretical. The UO_2 concentration is 0.7870 $\frac{g}{cm^2}$.

[9]These are exact calculations. However, stainless steel-thickness corrections to the nearest 0.001 in. will be adequate since smaller incremental changes will probably not be detectable.

APPENDIX B

Calculations for Go-No-Go UO_2-Stainless Steel Radiographic Reference Standards

A. Assumptions

1. The total UO_2 loading per plate will be 193.05 g (calculated from nominal 158 g U^{235} in U and 88% U in UO_2).
2. The core dimensions will be 18 in. (45.7 cm) long x 2.18 in. (5.54 cm) wide.
3. Clad thickness will be 0.005 in. ± 0.001 in.
4. The plate thickness will be 0.115 in. ± 0.001 in.
   (The above values are nominal from preliminary procurement specifications.)
5. The fabricated fuel plate density will be 94.4% of theoretical (observed through actual plate fabrication).
6. The theoretical densities of UO_2 and stainless steel are 10.96 $\frac{g}{cm^3}$ and 7.93 $\frac{g}{cm^3}$, respectively.

B. Nominal UO_2 Concentration

$$\frac{193.05 \text{ g } UO_2}{45.7 \text{ cm(L)} \times 5.54 \text{ cm(W)}} = 0.762 \frac{\text{g } UO_2}{cm^2}$$

C. Minimum and Maximum UO_2 Concentration (Tolerance of ± 5%)

$$0.762 - (0.762 \times 0.05) = 0.724 \frac{\text{g } UO_2}{cm^3} \text{ minimum}$$

$$0.762 + (0.762 \times 0.05) = 0.800 \frac{\text{g } UO_2}{cm^2} \text{ maximum}$$

D. Minimum X-Ray Attenuation for Acceptable Conditions Will be When:

1. Plate thickness is 0.114 in.
2. UO_2 concentration is 0.724 $\frac{g}{cm^2}$.
3. Clad thickness is minimum of 0.004 for total of 0.008 in. (As much as possible of the stainless steel is 94.4% of theoretical density.)

$0.724 \frac{g}{cm^2} \div [10.96 \frac{g}{cm^3} \times 0.944$ (% of theoretical density)$] \div 2.54 \frac{cm}{in.} =$ 0.0275 in. (effective thickness of UO_2 in fuel plate).

0.114 in. - 0.0275 in. of UO_2 - 0.008 in. clad = 0.0785 in. of stainless steel with density of 94.4% of theoretical.

0.0785 in. $\times 2.54 \frac{cm}{in.} \times [7.93 \frac{g}{cm^3} \times 0.944] = 1.494 \frac{g}{cm^2}$ of stainless steel.

The proper UO_2-stainless steel proportion for minimum core conditions will be $0.724 \frac{g}{cm^2}$ UO_2 and $1.494 \frac{g}{cm^2}$ stainless steel. The total weight will depend upon the area of the standard to be made.

Of course, 0.008 in. of stainless steel must be added as clad to simulate a fuel plate.

E. Maximum X-Ray Attenuation for Acceptable Conditions Will be When:

1. Plate thickness is 0.116 in.
2. UO_2 concentration is $0.800 \frac{g}{cm^2}$.
3. Clad thickness is maximum of 0.006 for total of 0.012 in. (As much as possible of the total stainless steel is 100% of theoretical density.)

$0.800 \frac{g\ UO_2}{cm^2} \div [10.96 \frac{g}{cm^3} \times 0.944$ (% of theoretical density)$] \div 2.54 \frac{cm}{in.} =$ 0.0304 in. UO_2.

0.116 in. - 0.0304 in. of UO_2 - 0.012 in. clad = 0.0736 in. of 94.4% dense stainless steel in the fuel core.

0.0736 in. $\times 2.54 \frac{cm}{in.} \times [7.93 \frac{g}{cm^3} \times 0.944] = 1.40 \frac{g}{cm^2}$ of stainless steel.

The proper UO_2-stainless steel proportion for maximum core condition will be $0.800 \frac{g}{cm^2}$ UO_2 and $1.40 \frac{g}{cm^2}$ stainless steel. The total weight will depend upon the area of the standard to be made.

Of course, 0.012 in. of stainless steel must be added as clad to simulate a fuel plate.

ORNL-3221
Metals, Ceramics, and Materials
TID-4500 (16th ed.)

DISTRIBUTION

1. Biology Library
2–3. Central Research Library
4. ORNL - Y-12 Technical Library, Document Reference Section
5–24. Laboratory Records
25. Laboratory Records, RC
26. G. M. Adamson, Jr.
27. R. J. Beaver
28. D. S. Billington
29. A. L. Boch
30. E. G. Bohlmann
31. E. S. Bomar, Jr.
32. B. S. Borie
33. C. J. Borkowski
34. R. B. Briggs
35. J. H. Cherubini
36. R. E. Clausing
37. J. H. Coobs
38. J. A. Cox
39. F. L. Culler
40. J. E. Cunningham
41. J. H. DeVan
42. R. G. Donnelly
43. D. A. Douglas, Jr.
44. J. H Frye, Jr.
45. J. H. Gillette
46. W. R. Grimes
47. J. P. Hammond
48. W. O. Harms
49. C. S. Harrill
50–54. M. R. Hill
55. E. E. Hoffman
56. A. Hollaender
57. A. S. Householder
58. H. Inouye
59. R. G. Jordon (Y-12)
60. M. T. Kelley
61. J. T. Lamartine
62. J. A. Lane
63. C. E. Larson
64. C. F. Leitten, Jr.
65. R. S. Livingston
66. A. L. Lotts
67. H. G. MacPherson
68. W. D. Manly
69–78. R. W. McClung
79. C. J. McHargue
80. A. J. Miller
81. E. C. Miller
82. K. Z. Morgan
83. J. P. Murray (K-25)
84. M. L. Nelson
85. A. R. Olsen
86. P. Patriarca
87. D. Phillips
88. H. W. Savage
89. L. D. Schaffer
90. J. L. Scott
91. H. E. Seagren
92. M. J. Skinner
93. G. M. Slaughter
94. C. O. Smith
95. J. A. Swartout
96. A. Taboada
97. E. H. Taylor
98. W. C. Thurber
99. A. M. Weinburg
100. J. R. Weir, Jr.
101. J. C. Wilson
102. C. E. Winters
103. A. A. Burr (consultant)
104. J. R. Johnson (consultant)
105. C. S. Smith (consultant)
106. R. Smoluchowski (consultant)

EXTERNAL DISTRIBUTION

107. W. H. Jens, APDA
108–127. A. A. Shoudy, APDA
128. R. C. Williams, APDA
129. L. A. Redecke, AEC, COO
130–131. Bruce Anderson, AEC, COO
132–133. David F. Cope, AEC, ORO
134–135. W. J. Larkin, AEC, ORO
136–137. G. M. Wensch, AEC, Washington
138. J. Simmons, AEC, Washington
139. Donald K. Stevens, AEC, Washington
140. D. E. Baker, GE, Hanford
141. Ersel Evans, GE, Hanford
142. J. L. Gregg, Cornell University
143. E. E. Stansbury, University of Tennessee
144–719. Given distribution as shown in TID-4500 (16th ed.) under Metals, Ceramics, and Materials Category (75 copies - OTS)